

# Ratiometric Two-Photon Fluorescent Probes for Mitochondrial Hydrogen Sulfide in Living Cells

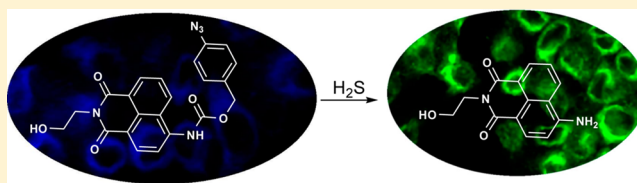
Xiu-Ling Liu,<sup>†</sup> Xiao-Jiao Du,<sup>‡</sup> Chun-Guang Dai,<sup>†</sup> and Qin-Hua Song<sup>\*,†</sup>

<sup>†</sup>Department of Chemistry, University of Science and Technology of China, Hefei 230026, P. R. China

<sup>‡</sup>School of Life Sciences, University of Science and Technology of China, Hefei 230027, P. R. China

**S** Supporting Information

**ABSTRACT:** Hydrogen sulfide (H<sub>2</sub>S) is an important signaling molecule with diverse biological roles. Various fluorescent probes for H<sub>2</sub>S with biological application have been developed. However, two-photon ratiometric imaging of mitochondrial H<sub>2</sub>S is scarce. In this paper, we report two ratiometric two-photon probes, AcHS-1 and AcHS-2, which employ 4-amino-1,8-naphthalimide as the fluorophore and 4-azidobenzyl carbamate as the H<sub>2</sub>S response site. These probes exhibit high selectivity toward H<sub>2</sub>S over biothiols and other reactive species, low detection limits of 50–85 nM, low cytotoxicity, and high stability under physiological conditions. Furthermore, through cell imaging with one-photon and two-photon microscopy, MCF-7 cells incubated with two probes show a marked change in emission color from blue to green in response to H<sub>2</sub>S. Cell images constraining with a mitochondrial dye reveal that AcHS-2 is a mitochondria-specific two-photon probe for H<sub>2</sub>S. These results show that AcHS-2 may find useful applications in biological research such as tracking mitochondrial H<sub>2</sub>S in living biological specimens.



## INTRODUCTION

Hydrogen sulfide (H<sub>2</sub>S) is a ubiquitous gaseous signaling molecule generated predominately from cysteine by two pyridoxal-5'-phosphate-dependent enzymes, cystathionine- $\beta$ -synthase and cystathionine- $\gamma$ -lyase, as well as by 3-mercapto-sulfurtransferase, in the cytosols and mitochondria of mammalian cells in relatively high concentration (10–100  $\mu$ M).<sup>1,2</sup> The significance of endogenous H<sub>2</sub>S has been recognized in a number of physiological and pathological processes.<sup>3,4</sup> H<sub>2</sub>S plays critical roles in regulating intracellular redox status and other fundational signaling processes involved in human health and disease.<sup>1,5</sup> Mitochondrial H<sub>2</sub>S has been shown to exert protective effects in oxidative stress leading to dysfunction and cell death,<sup>6–8</sup> and has become the focus of many research endeavors, including pharmacotherapeutic manipulation.<sup>9</sup>

To detect H<sub>2</sub>S in solutions and cells, a number of fluorescent probes<sup>10</sup> have been designed on the basis of reactions of H<sub>2</sub>S as a reductant to reduce azide or nitro group on masked fluorophore<sup>11</sup> or as a nucleophile to attack activated electrophiles,<sup>12</sup> precipitate metal salts,<sup>13</sup> or others.<sup>14</sup> Most of them are turn-on fluorescent probes, which are difficult to give quantitative information on the H<sub>2</sub>S concentration, since molecular emission intensity can be distinctly affected by photobleaching, microenvironments, and local probe concentration. Therefore, ratiometric probes for H<sub>2</sub>S are highly appealing owing to their ability in quantitative tracking. So far, a few ratiometric H<sub>2</sub>S probes have been reported.<sup>11d,f,12a,b,14b–e</sup> In addition, under one-photon excitation, short excitation wavelengths (<500 nm) limit applications of these probes with regard to deep-tissue imaging due to the shallow penetration

depth (<100  $\mu$ m). An attractive approach for the detection of H<sub>2</sub>S in organelles deep inside the tissues is through the use of two-photon microscopy (TPM), which employs near-IR photons as the excitation source, and it offers many advantages, including greater penetration depth (>500  $\mu$ m), localization of the excitation, and longer observation times.

Furthermore, selective tracking of H<sub>2</sub>S in an organelle such as mitochondria is crucial to elucidate the complex contributions of H<sub>2</sub>S in the physiological and pathological processes. However, five ratiometric fluorescent probes for mitochondrial H<sub>2</sub>S have been reported,<sup>11l,12a,b,14d,e</sup> and only one case<sup>11l</sup> is a two-photon probe. Therefore, this is still a strong need and requires challenging work to develop new ratiometric two-photon probes for mitochondrial H<sub>2</sub>S.

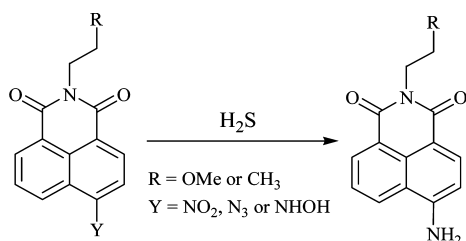
In this work, we developed two ratiometric fluorescent probes, AcHS-1 and AcHS-2, for detection of H<sub>2</sub>S. Moreover, we demonstrated that AcHS-2 is a new mitochondria-specific probe for H<sub>2</sub>S, and mitochondrial images can be achieved under both one-photon and two-photon excitations.

## RESULTS AND DISCUSSION

**1. Design and Synthesis of Probes.** 4-Amino-1,8-naphthalimide with intramolecular charge transfer (ICT) has been used as a fluorophore in H<sub>2</sub>S fluorescent probes,<sup>11e,g,12k</sup> but all these probes are the turn-on mode, as shown in Scheme 1. By modifying an ICT-state fluorophore to change the ICT property, the modified fluorophore could display a ratiometric spectral variation. If certain molecules such as H<sub>2</sub>S can induce a

Received: July 3, 2014



**Scheme 1. Reported Probes with a Turn-On Response Mode<sup>11e,g</sup>**

sensing reaction to remove this modifying group, the modified fluorophore would become a ratiometric two-photon fluorescent probe for the molecule. Based on this design strategy of ratiometric two-photon fluorescent probes, we designed two ratiometric probes for  $\text{H}_2\text{S}$ , using 4-amino-1,8-naphthalimide as the fluorophore and 4-azidobenzyl carbamate as a  $\text{H}_2\text{S}$  response site, shown in Scheme 2. As the azide is reduced to amine, probes may undergo a cleavage of the carbamate and release of the amino group. The 4-amino-1,8-naphthalimides with ICT states have large two-photon absorption cross sections.<sup>15</sup> Through introducing an electron-withdrawing carbamate group to convert the 4-amino donor into a weak donor, the ICT effect of the fluorophore is weakened to result in a blue-shift of fluorescence. On this basis that the thiolate-triggered reaction with the azide group would cleave the carbamate linkage and liberate the amine group,<sup>16,17</sup> we expect that a similar cleavage and release occurs for the new probes in the presence of  $\text{H}_2\text{S}$ .

The synthetic procedure for probes AcHS-1 and AcHS-2 is outlined in Scheme 3. Using 4-azidophenylmethyl bromide as a starting material, 4-azidophenylmethanol (**5**)<sup>18</sup> was prepared. *n*-Butylamine or aminoethanol was quickly added to a cloudy solution of 4-nitro-1,8-naphthalic anhydride<sup>19</sup> in ethanol. After being refluxed for 6 h under  $\text{N}_2$ , the solution was filtered, washed, and purified to give compound **6a**<sup>20</sup> or **6b**.<sup>21</sup> A stirred cloudy solution of **6a** or **6b** in ethanol was added to the solution of  $\text{SnCl}_2$  in concentrated hydrochloric acid at room temperature to afford compound **3**<sup>20</sup> or compound **4**.<sup>21</sup> A mixture of **3** or **4** and DMAP in toluene was added to a solution of triphosgene in toluene, heated to reflux for 3 h, diluted with  $\text{CH}_2\text{Cl}_2$ , and filtered. To the filtrate was added compound **5**,

stirred at room temperature for 3 h, and purified to give target products AcHS-1 and AcHS-2.

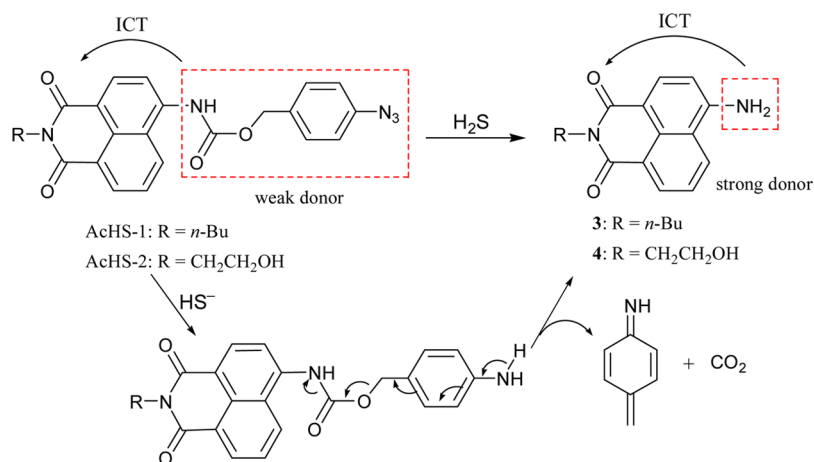
## 2. Spectral Response to $\text{H}_2\text{S}$ in Aqueous Solutions.

$\text{H}_2\text{S}$  is a weak acid in aqueous solutions ( $\text{p}K_{\text{a}1} = 7.04$ ,  $\text{p}K_{\text{a}2} = 11.96$ ),<sup>22</sup> equilibrating mainly with  $\text{HS}^-$  at physiological pH. For example, at pH 7.4 and temperature of  $37^\circ\text{C}$ , 18.5% of free hydrogen sulfide exists as  $\text{H}_2\text{S}$  molecule and the remainder is almost all hydrosulfide anion ( $\text{HS}^-$ ) with a negligible contribution of  $\text{S}^{2-}$ .<sup>23</sup> As the ion distribution of  $\text{Na}_2\text{S}$  is the same with that of  $\text{H}_2\text{S}$  in a neutral buffer solution,  $\text{Na}_2\text{S}$  was employed to replace  $\text{H}_2\text{S}$  in this work.

Parts a and c of Figure 1 show time-dependent UV/vis absorption spectra of  $10\ \mu\text{M}$  AcHS-1 and  $10\ \mu\text{M}$  AcHS-2 in the presence of 1 mM  $\text{Na}_2\text{S}$ , respectively. The absorption band in the range of 400–500 nm appears and increases, accompanying the decrease in the absorption peak at 370 nm. This change results in an isosbestic point at 400 nm, indicating the sensing reaction is a single transformation. The final absorption spectra show a larger red shift of 65 nm for AcHS-1 and 63 nm for AcHS-2 over those<sup>11</sup> of two probes reported (25 nm for SHS-M1 and 40 nm for SHS-M2). The color change of the solution from colorless to yellow can be observed by the naked eye (inset of Figure 1a).

The time-dependent fluorescent response of AcHS-1 or AcHS-2 to  $\text{H}_2\text{S}$  was also observed. The fluorescence spectra of AcHS-1 and AcHS-2 have a wide emission band (400–600 nm) with a peak at 468 nm for both AcHS-1 and for AcHS-2. With addition of  $\text{Na}_2\text{S}$ , the cleavage reaction of AcHS-1 or AcHS-2 would trigger and release the green fluorescent **3** or **4** with a stronger ICT-state emission ( $\Phi_{\text{f}}(\mathbf{3}) = 0.13$ ,  $\Phi_{\text{f}}(\mathbf{4}) = 0.12$  listed in Table 1). Consequently, the fluorescence emission intensity in the short wavelength region gradually decreases, accompanying appearance of a new emission band (475–650 nm) with a peak at 530 nm, exhibiting a ratiometric change with a large red-shift over 62 nm for both AcHS-1 and AcHS-2 as shown in Figure 1b,d. Fluorescence photos of AcHS-1 solutions without and with  $\text{Na}_2\text{S}$  are shown in the inset of Figure 1b. The ratio of  $F_{530}/F_{468}$  increases from 0.35, 0.28 to 3.37, 2.02 for AcHS-1 and AcHS-2, respectively, after incubation for 2 h.

Two-photon absorption cross sections ( $\delta$ ) were obtained by determining the two-photon absorption action spectra of probes and their sensing products **3** and **4**, listed in Table 1. The  $\delta_{\text{max}}$  values for AcHS-1 and AcHS-2 were 152 and 119

**Scheme 2. Proposed Sensing Mechanism of Probes, AcHS-1 and AcHS-2**

Scheme 3. Synthetic Route of Probes AcHS-1 and AcHS-2

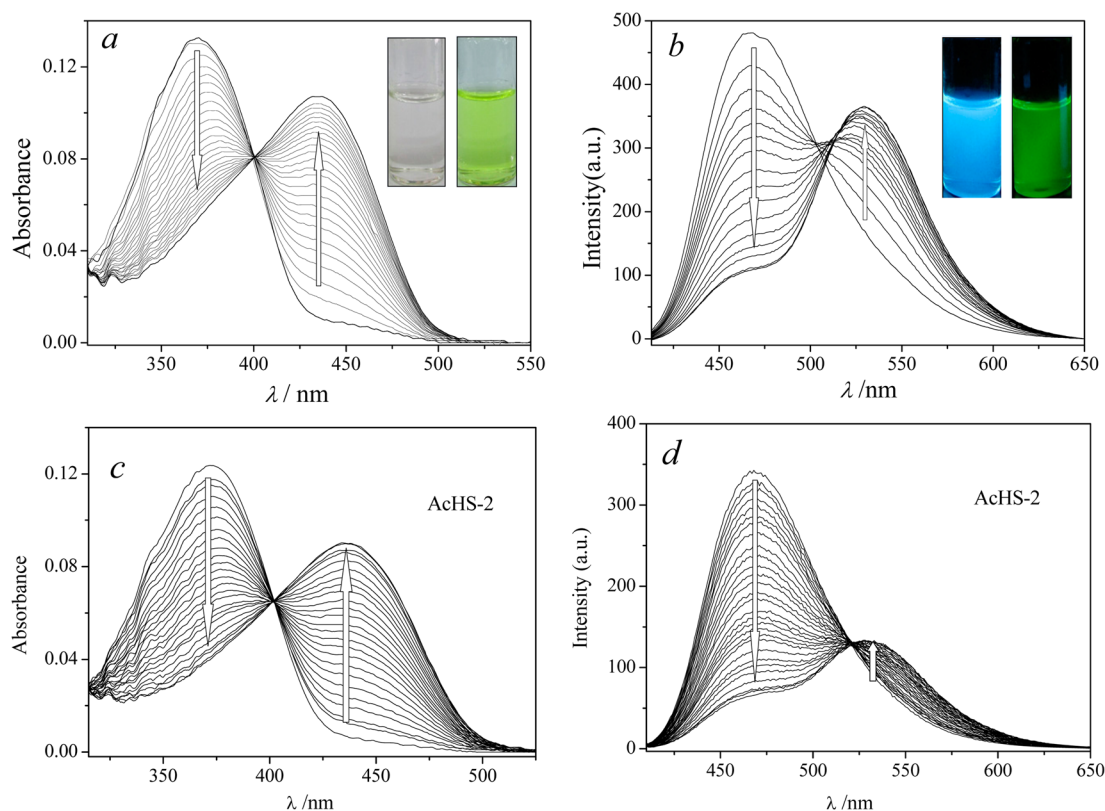
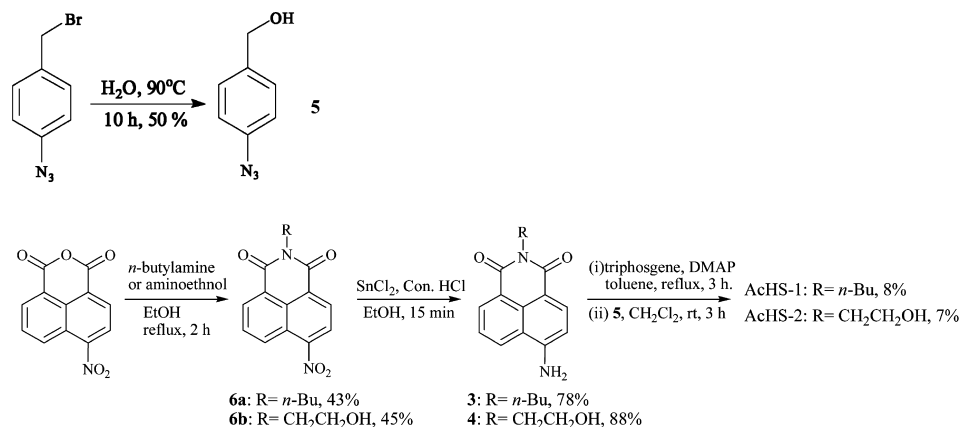


**Figure 1.** Time-dependent UV/vis absorption (a, c) and fluorescence spectra (b, d) of 10  $\mu\text{M}$  AcHS-1 or AcHS-2 in EtOH/PBS (v/v1:4, pH 7.0) response toward Na<sub>2</sub>S (1 mM), respectively, excitation at 410 nm. Insets in (a) and (b): photograph for the solution color and the fluorescent changes of AcHS-1 without and with Na<sub>2</sub>S in the buffer solution, respectively.

GM, respectively, and lower than those of **3** and **4** (207 and 218 GM, respectively). The higher two-photon absorption cross-sections for **3** and **4** over the probes can be attributed to their enhanced donor, 4-amino group.

**3. Sensing Mechanism.** To further confirm the validity of the proposed sensing mechanism, the sensing reaction of AcHS-1 to Na<sub>2</sub>S in DMSO-*d*<sub>6</sub> was analyzed by means of NMR spectroscopy, with partial <sup>1</sup>H NMR spectra shown in Figure 2. As shown in Figure 2a, a characteristic single peak at 5.48 ppm was assigned to the proton (H<sup>g</sup>) of AcHS-1, and the single peak was not observed from the <sup>1</sup>H NMR spectrum of the reaction mixture of AcHS-1 and Na<sub>2</sub>S (Figure 2b). In this field region, most of the emerging peaks for <sup>1</sup>H NMR spectrum of the reaction mixture match with those of compound **3**. Hence, the

sensing reaction of AcHS-1 with Na<sub>2</sub>S could occur via the cleavage of azido-based carbonate moiety and release of **3**. Furthermore, the main H<sub>2</sub>S-induced product is confirmed to be compound **3** by coinjection HPLC analysis. As shown in Figure 3, with increasing reaction time, the chromatogram peak at 19.5 min of AcHS-1 decreases with a simultaneous increase for a new peak at 3.2 min, which is assigned to compound **3**.

**4. Sensitivity and Selectivity. Detection Limits.** The fluorescence spectra of 0.2  $\mu\text{M}$  AcHS-1 in EtOH/PBS (v/v1:4, pH 7.0) in the presence of various concentrations of Na<sub>2</sub>S from 0 to 6  $\mu\text{M}$  were collected and are shown in Figure S1 (Supporting Information). A linear regression curve was then fitted according to the ratio of fluorescence intensity at *F*<sub>530</sub>/*F*<sub>465</sub> in the range of [Na<sub>2</sub>S] from 0 to 6  $\mu\text{M}$ . The detection limit

Table 1. Photophysical Data for AcHS-1, AcHS-2, 3, and 4<sup>a</sup>

compd	$\lambda_{\text{abs}} (10^{-4} \epsilon)^b$	$\lambda_{\text{fl}}^c$	$\Phi^d$	$\lambda_{\text{max}}^e$	$\delta_{\text{max}}^f$
AcHS-1	370 (1.34)	468	0.15	740	152
3	435 (1.20)	530	0.13	820	207
AcHS-2	373 (1.34)	468	0.10	730	119
4	436 (1.18)	530	0.12	800	218

<sup>a</sup>Measurements were performed in EtOH/PBS (v/v1:4, 100 mM, pH 7.0), unless otherwise noted. <sup>b</sup> $\lambda_{\text{max}}$  of the one-photon absorption spectra in nm. The values in parentheses are molar extinction coefficients in  $\text{M}^{-1} \text{cm}^{-1}$ . <sup>c</sup>Fluorescence maxima. <sup>d</sup>Fluorescence quantum yields,  $\pm 10\%$ . <sup>e</sup> $\lambda_{\text{max}}$  of the two-photon absorption action spectra in nm, measured in acetonitrile. <sup>f</sup>Peak two-photon absorption action cross sections in GM ( $1 \text{ GM} = 10^{-50} \text{ m}^4 \text{ s photon}^{-1}$ ),  $\pm 10\%$ , measured in acetonitrile.

( $3N/k$ ) was determined to be  $0.05 \mu\text{M}$ , where  $N$  is the standard deviation of the intercept and  $k$  is the slope of the fitting straight line in the inset of Figure S1 (Supporting Information). Similarly, the detection limit of AcHS-2 was obtained,  $0.085 \mu\text{M}$  (Figure S2, Supporting Information).

**Selectivity.** The selectivity of probes was determined for  $\text{H}_2\text{S}$  over other biologically relevant species, including reactive sulfide (cysteine (Cys), glutathione (GSH),  $\text{SCN}^-$ ), reductants ( $\text{S}_2\text{O}_3^{2-}$ ,  $\text{SO}_3^{2-}$ , ascorbic acid (Vc),  $\text{S}_2\text{O}_4^{2-}$ ), reactive oxygen ( $\text{HClO}$ ,  $\text{H}_2\text{O}_2$ ,  $t\text{-BuOOH}$ ), nitrogen species ( $\text{NO}_2^-$ ), and metal ions ( $\text{Ca}^{2+}$ ,  $\text{Na}^+$ ,  $\text{K}^+$ ). Both AcHS-1 and AcHS-2 displayed a marked response for  $\text{H}_2\text{S}$  over other biological relevant species. As shown in Figure 4, pronounced fluorescence changes were observed from the solution with  $\text{H}_2\text{S}$ , and no significant change occurred for solutions with other analytes. The fluorescence intensity ratios ( $F_{530}/F_{468}$ ) for  $\text{Na}_2\text{S}$  over other analytes were 8–17-fold for AcHS-1 and 5–7-fold for AcHS-2. Meanwhile, the naked-eye color of probe solutions changed from colorless to yellow, and the emission color from blue to green only in the presence of  $\text{Na}_2\text{S}$  (inset of Figure 4left).

**5. pH Effect on Fluorescent Response and Stability of Probes.** To examine the pH-dependent fluorescent response, fluorescence intensities of the sensing reaction in different

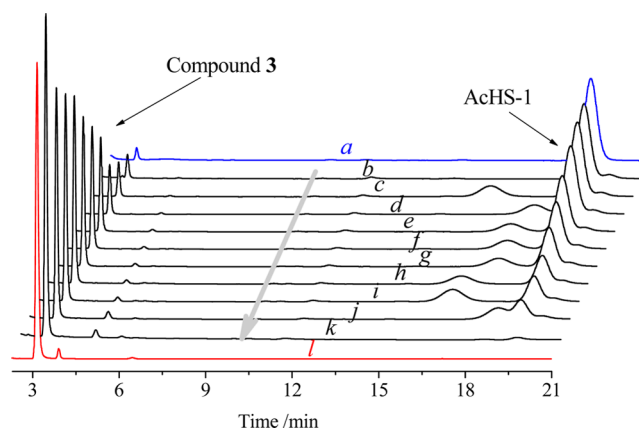


**Figure 3.** Time-dependent HPLC profiles of AcHS-1 ( $10 \mu\text{M}$ ) in the presence of  $\text{Na}_2\text{S}$  ( $1 \text{ mM}$ ) in methanol/water ( $1:1, \text{v/v}$ ). The eluent is a methanol/water solvent mixture ( $80:20, \text{v/v}$ ), monitored at  $254 \text{ nm}$  (a,  $0 \text{ min}$ ; b,  $5 \text{ min}$ ; c,  $10 \text{ min}$ ; d–j, interval of  $20 \text{ min}$ ; k,  $4 \text{ h}$ ; l, neat compound 3). Retention times:  $3.2 \text{ min}$  (product 3),  $19.5 \text{ min}$  (AcHS-1).

solutions (pH 2.0–10.0) were measured (Figure 5a). The fluorescence spectra of probes AcHS-1 and AcHS-2 were recorded at various pH solutions (EtOH/PBS (v/v1:4)). The pH-dependence response was estimated by the fluorescence intensity ratio at  $F_{530}/F_{468}$  under excitation at  $410 \text{ nm}$ . Under neutral or alkaline conditions (pH  $> 6$ ), probes AcHS-1 and AcHS-2 can respond to  $\text{H}_2\text{S}$  with a remarkable fluorescence change, while no obvious response was observed in acidic solutions (pH  $< 5$ ).

For the pH effect on the stability of the probes, UV/vis absorption spectra of AcHS-1 and AcHS-2 in various solutions from pH 2 to 10 were recorded, respectively (Figure 5b). The stability of probes AcHS-1 and AcHS-2 were estimated by measuring the absorbance at  $370 \text{ nm}$  for absorption peak of the probes and  $436 \text{ nm}$  for absorption peak of compound 3 in various pH solutions (Figure 5b). As shown in Figure 5b, no significant change at the two wavelengths,  $370$  and  $436 \text{ nm}$ , was

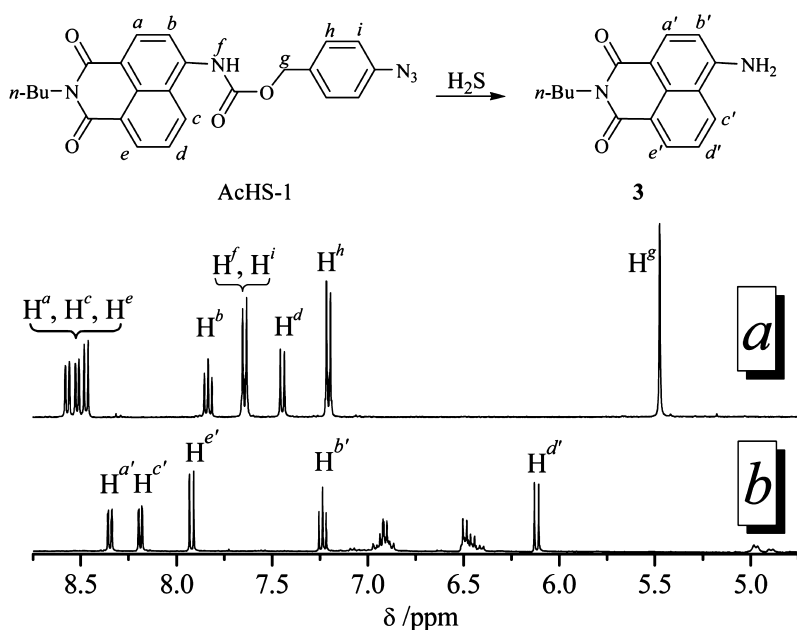


**Figure 2.** Partial  $^1\text{H}$  NMR ( $400 \text{ MHz}$ ) spectra of AcHS-1 (a), AcHS-1 and  $\text{Na}_2\text{S}$  (molar ratio  $1:10$ ) in  $\text{DMSO}-d_6$  (b).

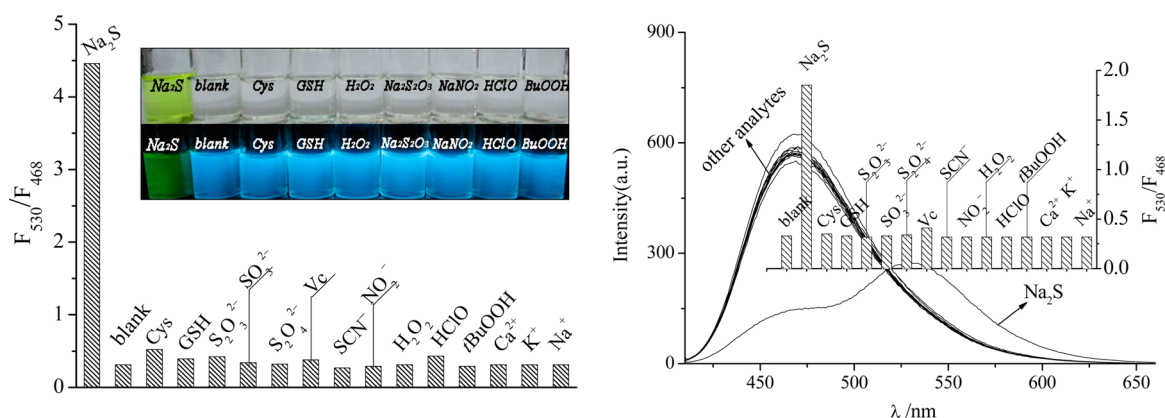


**Figure 4.** Left: Fluorescence responses of AcHS-1 (10 μM) to various analytes (1 mM) at  $F_{530}/F_{468}$  in EtOH/PBS (v/v:4, pH 7.0). Inset: photos of naked-eye and fluorescent responses of AcHS-1 to various analytes. Right: fluorescence spectra of AcHS-2 (10 μM) in the presence of various analytes (1 mM) in the buffer solution. Inset: the corresponding fluorescence response, under excitation at 400 nm, incubation for 2 h.

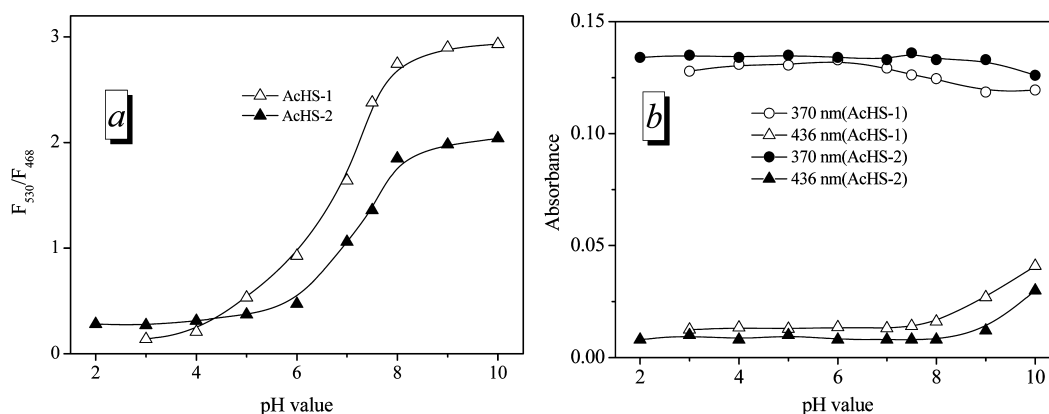


**Figure 5.** (a) Plot of the ratio of  $F_{530}/F_{468}$  for AcHS-1 (10 μM) and AcHS-2 (10 μM) vs pH value in the presence of 1 mM  $\text{Na}_2\text{S}$ . (b) Absorbance at 370 and 436 nm of 10 μM AcHS-1 and AcHS-2, in different pH solutions, incubation for 2 h.

observed at pH 2–8. This indicates that the probes are stable in pH 2–8 solutions. In addition, the stability of probes under the physiological condition was also estimated by tracking their UV/vis absorption spectra in a PBS buffer (pH 7.4) for 10 h (Figure S3, Supporting Information). Their absorption spectra display no significant change. These results show that AcHS-1 and AcHS-2 not only can detect  $\text{H}_2\text{S}$  but also are considerably more stable under physiological conditions (pH 6–8).

**6. Fluorescence Imaging of Living Cells. Cell Toxicity of Probes.** In order to detect  $\text{H}_2\text{S}$  in living MCF-7 cells, a MTT experiment was carried out to assess the cytotoxicity of the probes. In the MTT assays, MCF-7 cells were dealt with probes in different concentrations from 5 to 20 μM for 24 h. The results show that the probes have low toxicity to cultured cells under the experimental conditions (Figure 6) and the cell viability is 93% and 89% for AcHS-1 and AcHS-2 at 5 μM, respectively.

**Fluorescent Imaging of Cells.** The MCF-7 cells were placed in a 96-well plate and treated with 5 μM AcHS-1 or AcHS-2 for 1 h, and then the cells in one well were incubated with 0.5 mM  $\text{Na}_2\text{S}$  for an additional 1 h. Two types of cells were washed with PBS three times for confocal fluorescence microscopy (Figures 7 and 8). As shown in Figure 7, cells incubated alone with AcHS-1 display blue emission collected from the blue channel (408–500 nm), and cells costained by AcHS-1 and  $\text{Na}_2\text{S}$  emit green fluorescence collected from the green channel (500–650 nm) under one-photon excitation of 405 nm. Upon two-

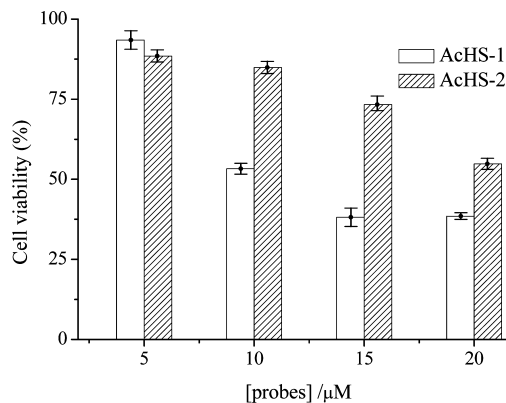


**Figure 6.** MTT assay of MCF-7 cells in the presence of different concentrations of probes.

photon excitation at 750 nm, cells stained alone with AcHS-1 emitted similar fluorescence, shown in Figure S4 (Supporting Information).

Similarly, cells stained by AcHS-2 with and without  $\text{Na}_2\text{S}$  emit different-color fluorescence (Figure 8a–f). Moreover, upon two-photon excitation at 750 nm for cells stained alone with AcHS-2 as shown in Figure S4 (Supporting Information) and 800 nm for cells costained by AcHS-2 and  $\text{Na}_2\text{S}$  (Figure 8g–i), confocal fluorescence microscopy collects similar emissions from the two channels. These results show that

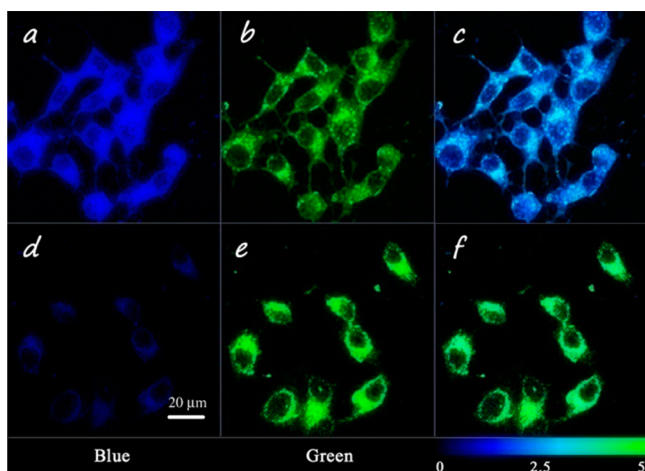


**Figure 7.** Confocal fluorescence images of MCF-7 cells incubated with 5  $\mu$ M AHS-1 for 1 h (a–c) and then 0.5 mM  $\text{Na}_2\text{S}$  for 1 h (d–f). Images were acquired using 405 nm excitation and emission channels of 408–500 nm (blue) and 500–650 nm (green). Cells shown are representative images from replicate experiments ( $n = 3$ ).

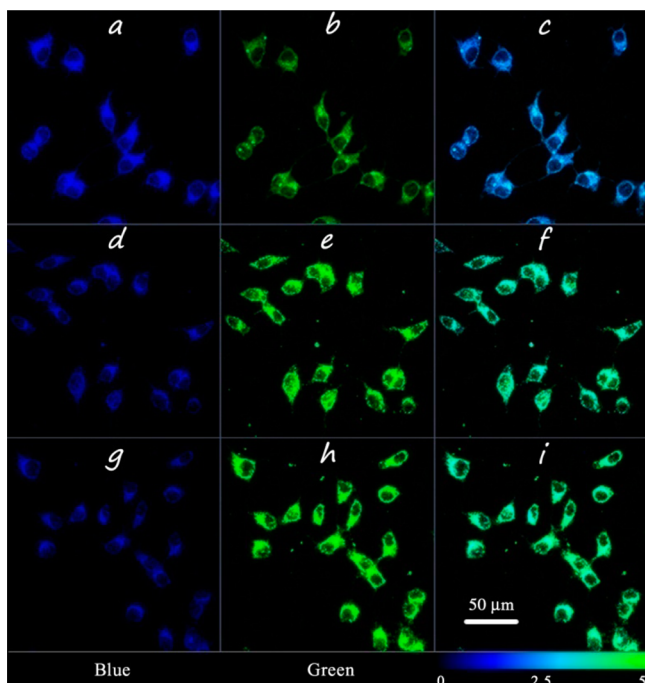


**Figure 8.** Confocal fluorescence images of MCF-7 cells incubated with 5  $\mu$ M AHS-2 for 1 h (a–c) and then 0.5 mM  $\text{Na}_2\text{S}$  for 1 h, under 405 nm excitation (d–f) and 800 nm excitation (g–i). Images were acquired with emission channels of 408–500 nm (blue) and 500–650 nm (green). Cells shown are representative images from replicate experiments ( $n = 3$ ).

AcHS-2 can detect  $\text{H}_2\text{S}$  in live cells by cellular imaging under both one-photon and two-photon excitation.

From the ratiometric fluorescence images shown in Figures 7 and 8, the values of  $F_{\text{green}}/F_{\text{blue}}$ , the ratio of the relative emission intensity of 500–650 nm (green) and 408–500 nm (blue), showed large changes for systems between with and without  $\text{Na}_2\text{S}$  (Figure 9). The values of  $F_{\text{green}}/F_{\text{blue}}$  for MCF-7 cells stained alone with AcHS-1 and AcHS-2 were 0.31 and 0.38, and the values for the cells incubated with additional  $\text{Na}_2\text{S}$  increased

to 3.9 and 2.9, respectively. This indicates that two probes can serve as ratiometric fluorescent probes for  $\text{H}_2\text{S}$  in cells.

The cell images above show that the probes could localize at mitochondria. To further investigate the mitochondria localization of AcHS-2, a commercially available mitochondrial dye (MitoTracker Red CMXRos)<sup>24</sup> was employed for a colocalization study. MCF-7 cells were stained with AcHS-2 and the MitoTracker in succession and observed under the confocal fluorescence microscopy by one- and two-photon images. As shown in Figure 10, the green-channel images for AcHS-2 with and without  $\text{Na}_2\text{S}$  merged well with the red-channel images for MitoTracker dye under one-photon excitation (Figure 10d, h). The colocalization assay with the mitochondrial dye and AcHS-2 revealed that fluorescence of AcHS-2 was colocalized with that of the mitochondrial dye, and the overlap coefficients were 0.79 for the cells without  $\text{Na}_2\text{S}$  (Figure 10d) and 0.71 for the cells with  $\text{Na}_2\text{S}$  (Figure 10h). Upon one- and two-photon excitation at 375 and 750 nm, confocal images of MCF-7 cells costained by AcHS-2 and another mitochondrial specific dye MitoTracker Deep Red FM<sup>24</sup> displayed excellent overlap between the green-channel images for AcHS-2 and the red-channel images for the MitoTracker dye under one-photon excitation (Figure S5, Supporting Information). The overlap coefficients between the green channel and the red channel were 0.80 for one-photon image (Figure S5d, Supporting Information), 0.87 for two-photon image (Figure S5h, Supporting Information). The high overlap coefficients indicate that AcHS-2 can accumulate in the mitochondria.

It is well-known that the commercial dyes for mitochondria are cationic and can accumulate in the mitochondria due to the negatively charged surface of the mitochondrial membrane. In this work, however, two probes are electroneutral, and the difference in structures is *N*-*n*-butyl for AcHS-1 and *N*-(2-hydroxyethyl) for AcHS-2. By comparing cell images of two probes, we found that all images of the cells stained with AcHS-2 were brighter than those stained with AcHS-1. Hence, we inferred that the hydrogen bonds formed between the hydroxyl group (and 4-amino) with mitochondrial membrane may be the reason why the probes, especially AcHS-2, accumulate in the mitochondria.

## CONCLUSION

In summary, we developed two ratiometric two-photon fluorescent probes based on an ICT-state fluorophore, 4-amino-1,8-naphthalimide. By modifying the fluorophore with an electron-withdrawing group, 4-azidophenyl methoxy carbonyl, to convert the amino group into a weak donor, also as the site of the sensing reaction to  $\text{H}_2\text{S}$ , the resulting probe molecules display a new ICT property, affording ratiometric spectral changes and achieving two-photon excitation. The two fluorescent probes can be used for specific ratiometric sensing of  $\text{H}_2\text{S}$  upon both one-photon and two-photon excitation. The study provided a design strategy of ratiometric two-photon fluorescent probes. Furthermore, cell-imaging experiments reveal that AcHS-2 is a new mitochondria-specific and emission-ratiometric two-photon probe for  $\text{H}_2\text{S}$ . The new probe is promising to be utilized in a variety of chemical and biological applications.

## EXPERIMENTAL SECTION

**Instrumentation and Methods.**  $^1\text{H}$  and  $^{13}\text{C}$  NMR spectra were recorded on an NMR spectrometer operating at 400 or 300 and 75 MHz, respectively. FT-IR spectra were carried out with an infrared

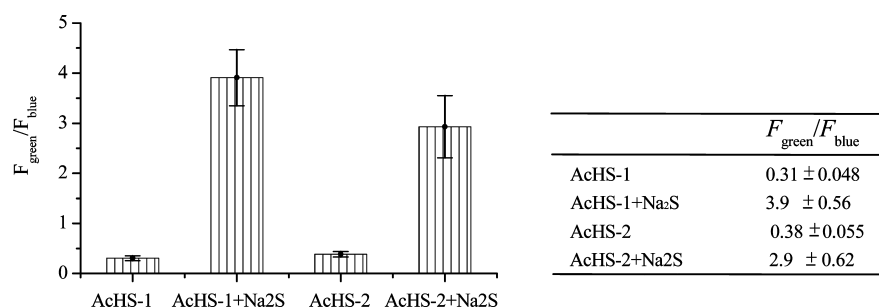


**Figure 9.** Average intensity ratios ( $F_{\text{green}}/F_{\text{blue}}$ ) for AcHS-1, AcHS-1/Na<sub>2</sub>S (Figure 7cf), AcHS-2, and AcHS-2/Na<sub>2</sub>S (Figure 8cf).

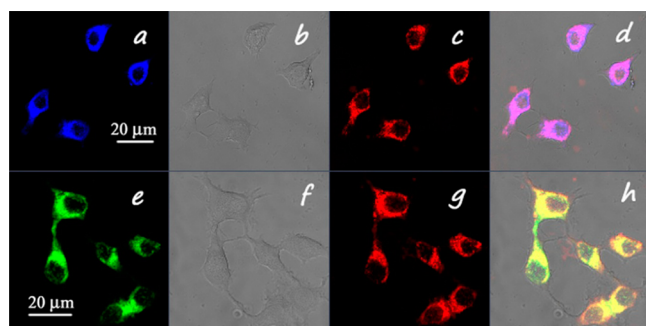


**Figure 10.** Confocal fluorescence images of MCF-7 cells costained by AcHS-2 (5  $\mu$ M, 1 h) and MitoTracker Red CMXRos (0.5  $\mu$ M, 30 min) without (a–d) and with 0.5 mM Na<sub>2</sub>S (e–h): (a, e) fluorescence images obtained with band paths of 408–500 nm for cells incubated by only AcHS-2 and 500–650 nm for cells incubated by AcHS-2 and Na<sub>2</sub>S, upon excitation of AcHS-2 at 405 nm; (b, f) bright-field images; (c, g) images from a band path of 600–705 nm; (d, h) merged images of (a), (b) and (c) or (e), (f) and (g).

spectrometer. High-resolution mass spectrometry data were obtained with a FTMS spectrometer or a LC–TOF MS spectrometer. UV–vis absorption spectra and fluorescence spectra were recorded at room temperature on a UV/vis spectrometer and a spectrofluorophotometer, respectively. The reaction mixtures of the probe with H<sub>2</sub>S were analyzed by a HPLC with a C-18 reversed-phase column.

**General Procedure for Spectral Measurements.** Sample solutions of AcHS-1 or AcHS-2 (10  $\mu$ M, 2.5 mL) in a buffer solution (0.01 M pH 7.0 phosphate buffer/EtOH = 4/1) were prepared in a quartz cuvette (1 cm  $\times$  1 cm). Various 250 mM analytes were prepared in pH 7.0 phosphate buffer, and a 10  $\mu$ L of the analyte was added to sample. Water for sample preparation was purified with a Millipore system. All pH values were measured on a pH meter. The fluorescence quantum yields ( $\Phi_f$ ) of probes and compound 3 and 4 were determined in spectroscopic-grade solvents. The optical density of the dilute solution of all compounds (the references AcHS-1 and AcHS-2 and compounds 3 and 4) was around 0.05 at the excitation wavelength, using fluorescein ( $\Phi_f = 0.90$  in 0.1 N NaOH)<sup>25</sup> solution and quinine sulfate ( $\Phi_f = 0.54$  in 0.1 N H<sub>2</sub>SO<sub>4</sub>)<sup>26</sup> as references at excitation wavelengths of 436 and 370 nm, respectively.

**Measurements of Two-Photon Absorption Cross Section ( $\delta$ ).** Two-photon absorption (TPA) experiments were carried out on the open-aperture Z-scan setup<sup>27</sup> using a femtosecond laser with a pulse duration of 140 fs and 80 MHz repetition rate. The thermal heating of the sample with high repetition-rate laser pulse was removed by the use of a mechanical chopper running at 1 kHz.<sup>28</sup> Nonlinear absorption coefficient  $\beta$  was measured by the open-aperture Z-scan technique. For the open aperture, the normalized transmittance as a function of the position along the  $z$  axis can be written as eq 1

$$Tz = \sum_{m=0}^{\infty} \frac{[-q(z)]^m}{(m+1)^{3/2}}, \text{ where } q(z) = \frac{\beta I_0 L_{\text{eff}}}{[1 + (z/z_0)^2]\alpha} \quad (1)$$

where  $I_0$  is the input intensity at the focus  $z = 0$ ,  $L$  is the sample length,  $\alpha$  is the linear absorption coefficient, and  $\beta$  is the two-photon absorption coefficient.  $z_0 = \pi \omega_0^2/\lambda$  is the Rayleigh diffraction length, and  $\omega_0$  is the radius of beam at focus. Thus, once an open-aperture Z-scan is performed, the nonlinear absorption coefficient  $\beta$  can be unambiguously deduced. Furthermore, the molecular TPA cross-section ( $\sigma$ ) could be determined by using the following relationship<sup>29</sup>

$$\delta = (h\nu\beta \times 10^{-3})/(N_A d) \quad (2)$$

where  $h$  is the Planck's constant,  $\nu$  is the frequency of input intensity,  $N_A$  is the Avogadro constant, and  $d$  is the concentration of the sample.

**Determination of Detection Limits.** The detection limit was calculated on the basis of the method reported in the literature.<sup>30</sup> The fluorescence emission spectra of probes were measured three times and the standard deviation of a blank measurement was achieved. The ratio of fluorescence intensity at  $F_{530}/F_{465}$  vs the concentration of Na<sub>2</sub>S was plotted. The detection limit was calculated by using the equation detection limit =  $3N/k$ , where  $N$  is the standard deviation of the blank measurement  $k$  is the slope of the plot.

**Cell Cultures and MTT Assays.** MCF-7 cells were seeded in DMEM (Dulbecco's modified Eagle's medium) supplemented with 10% FBS (fetal bovine serum) in an atmosphere of 5% CO<sub>2</sub> and 95% air at 37  $^{\circ}$ C. Before the experiment, the cells were placed in a 96-well plate, followed by addition of various concentrations of probes. The final concentrations of probes vary from 0 to 20  $\mu$ M. The cells were then incubated at 37  $^{\circ}$ C in an atmosphere of 5% CO<sub>2</sub> and 95% air for 24 h, followed by MTT assays ( $n = 4$ ).

**Cell-Imaging Experiments.** MCF-7 cells cultured under the above condition were employed for cell-imaging experiments. The imaging of MCF-7 cells was performed by a laser scanning confocal fluorescence microscope (Zeiss LSM 510 Meta NLO). The cells were treated initially with 5  $\mu$ M AcHS-2 for 1 h. Then, Na<sub>2</sub>S (0.5 mM) was added to the incubation medium, and the cells were incubated for 1 h. The excitation wavelength was 375 or 405 nm and 750 or 805 nm for one-photon and two-photon assays, respectively. Fluorescence signals were collected from the blue channel (420–550 nm) and the green channel (500–640 nm), respectively.

The colocalization experiment was carried out at the monoemission mode. MCF-7 cells were stained by AcHS-2 (5  $\mu$ M, 1 h) and MitoTracker Red CMXRos (0.5  $\mu$ M, 30 min) or MitoTracker Deep Red FM (1  $\mu$ M, 30 min) in sequence. The images for AcHS-2 were collected with band paths of 408–500 nm for cells stained by only AcHS-2 or 500–650 nm for cells stained by AcHS-2 and Na<sub>2</sub>S in succession, while the images for two mitochondria dyes were collected with a band path of 600–705 nm or 665–750 nm upon excitation at 578 or 633 nm, respectively.

**Materials.** Unless stated otherwise, all chemical reagents were purchased from commercial sources and used without further purification. Solvents of technical quality were distilled prior to use. Water for preparation of solutions was purified with a Millipore water system.

**Synthesis of 4-Azidophenylmethanol (5).**<sup>18</sup> 4-Azidophenylmethyl bromide (1.3 g, 0.6 mmol) was suspended in water (5 mL). Under nitrogen atmosphere, the mixture was stirred overnight at 90  $^{\circ}$ C and then cooled at room temperature and extracted with ethyl

acetate. The organic phase was dried with anhydrous  $\text{Na}_2\text{SO}_4$  and concentrated to dryness, the residue was purified using flash chromatography (EtOAc/petroleum ether, 1:4 v/v), and **5** was obtained as a yellow oil (455 mg, 50%):  $^1\text{H}$  NMR ( $\text{CDCl}_3$ , 400 MHz)  $\delta$  7.35 (d,  $J$  = 8.1 Hz, 2H), 7.02 (d,  $J$  = 8.1 Hz, 2H), 4.67 (s, 2H) ppm.

**Synthesis of *N*-*n*-Butyl-4-nitro-1,8-naphthalimide (6a).**<sup>20</sup> *n*-Butylamine (200  $\mu\text{L}$ , 1.6 mmol) was quickly added to a cloudy solution of 4-nitro-1,8-naphthalic anhydride<sup>19</sup> (340 mg, 1.4 mmol) in ethanol (7 mL). After being refluxed for 6 h under  $\text{N}_2$ , the reaction was allowed to cool to room temperature, filtered, and washed with cool ethanol (2 mL). The residue was purified using flash chromatography (EtOAc/petroleum ether, 1:10 v/v), and compound **6a** was obtained as a pale yellow solid (180 mg, 43%):  $^1\text{H}$  NMR ( $\text{CDCl}_3$ , 400 MHz)  $\delta$  8.85 (dd,  $J$  = 8.7 Hz,  $J$  = 1.0 Hz, 1H), 8.74 (dd,  $J$  = 7.3 Hz,  $J$  = 1.0 Hz, 1H), 8.70 (d,  $J$  = 8.0 Hz, 1H), 8.41 (d,  $J$  = 8.0 Hz, 1H), 7.98 (dd,  $J$  = 8.7 Hz,  $J$  = 7.3 Hz, 1H), 4.20 (t,  $J$  = 7.5 Hz, 2H), 1.72 (m, 2H), 1.46 (m, 2H), 0.99 (t,  $J$  = 7.3 Hz, 3H) ppm.

**Synthesis of *N*-*n*-Butyl-4-amido-1,8-naphthalimide (3).**<sup>20</sup> A stirred cloudy solution of **6a** (140 mg, 0.47 mmol) in ethanol (5 mL) was added dropwise to the solution of  $\text{SnCl}_2 \cdot 2\text{H}_2\text{O}$  (677 mg, 3 mmol) in concentrated hydrochloric acid (1 mL) at room temperature for 15 min. The reaction was quenched with aqueous 10%  $\text{Na}_2\text{CO}_3$  and filtered. After being washed with water ( $3 \times 10$  mL), the residue was dried in vacuo to afford compound **3** (98 mg, 78%):  $^1\text{H}$  NMR ( $\text{DMSO}-d_6$ , 400 MHz)  $\delta$  8.61 (d,  $J$  = 8.4 Hz, 1H), 8.42 (d,  $J$  = 7.3 Hz, 1H), 8.18–8.20 (m, 1H), 7.43–7.67 (m, 1H), 7.43 (s, 2H), 6.84 (d,  $J$  = 8.4 Hz, 1H), 4.00 (t,  $J$  = 7.2 Hz, 2H), 1.54–1.62 (m, 2H), 1.28–1.38 (m, 2H), 0.93 (t,  $J$  = 7.6 Hz, 3H) ppm;  $^{13}\text{C}$  NMR ( $\text{DMSO}-d_6$ , 75 MHz)  $\delta$  13.7, 19.8, 29.8, 40.0, 107.5, 108.1, 119.3, 121.8, 123.9, 129.2, 129.6, 130.9, 133.9, 152.6, 162.9, 163.7; IR (Nujol)  $\bar{\nu}$  3431 (s), 3355 (s), 2954 (m), 1636 (s), 1576 (s), 2372 (s), 771  $\text{cm}^{-1}$  (s); UV/vis (pH 7.0 PBS buffer)  $\lambda_{\text{max}}$  ( $\epsilon$ ) 435 nm ( $12000 \text{ mol}^{-1} \text{ dm}^3 \text{ cm}^{-1}$ ); FTMS (ESI) calcd for  $\text{C}_{16}\text{H}_{17}\text{N}_2\text{O}_2$  [ $\text{M}^+$ ] 269.1284, found 269.1281.

**Synthesis of AcHS-1.** A mixture of **3** (134 mg, 0.5 mmol) and DMAP (192 mg, 1.50 mmol) in toluene (7.5 mL) was added dropwise to a solution of triphosgene (152 mg, 0.5 mmol) in toluene. The resulting solution was heated to reflux for 3 h. After being cooled to room temperature, the reaction mixture was diluted with  $\text{CH}_2\text{Cl}_2$  (6 mL) and filtered. To the filtrate was added **5** (100 mg, 0.55 mmol), and the solution was stirred at room temperature for 3 h. The reaction was then concentrated and purified by flash column chromatography (EtOAc/petroleum ether, 1:2 v/v) to afford AcHS-1 as a pale yellow solid (15 mg, 6.8%):  $^1\text{H}$  NMR ( $\text{DMSO}-d_6$ , 400 MHz)  $\delta$  8.56 (d,  $J$  = 8.0 Hz, 1H), 8.52 (d,  $J$  = 8.8 Hz, 1H), 8.47 (d,  $J$  = 8.4 Hz, 1H), 7.83 (t,  $J$  = 8.0 Hz, 1H), 7.64 (d,  $J$  = 8.4 Hz, 2H), 7.45 (d,  $J$  = 8.4 Hz, 1H), 7.21 (d,  $J$  = 8.4 Hz, 2H), 5.48 (s, 2H), 4.04 (t,  $J$  = 7.4 Hz, 2H), 1.61 (m, 2H), 1.35 (m, 2H), 0.94 (t,  $J$  = 7.4 Hz, 3H) ppm;  $^{13}\text{C}$  NMR ( $\text{DMSO}-d_6$ , 75 MHz)  $\delta$  13.7, 19.8, 29.6, 40.0, 66.0, 117.1, 118.1, 119.2, 122.2, 123.8, 126.3, 128.3, 129.2, 130.2, 130.9, 131.6, 133.1, 139.3, 140.6, 153.9, 162.9, 163.4; IR (Nujol)  $\bar{\nu}$  3294 (s), 2959 (s), 2115 (m), 1692 (s), 1650 (s), 1538 (s), 1248 (s), 772 (s)  $\text{cm}^{-1}$ ; UV/vis (pH 7.0 PBS buffer)  $\lambda_{\text{max}}$  ( $\epsilon$ ) 370 nm ( $13400 \text{ mol}^{-1} \text{ dm}^3 \text{ cm}^{-1}$ ); FTMS (ESI) calcd for  $\text{C}_{24}\text{H}_{22}\text{N}_5\text{O}_4$  [ $\text{M}^+$ ] 444.1666, found 444.1664.

**Synthesis of *N*-(2-Hydroxyethyl)-4-nitro-1,8-naphthalimide (6b).**<sup>21</sup> Aminoethanol (80  $\mu\text{L}$ , 1.2 mmol) was quickly added to a cloudy solution of 4-nitro-1,8-naphthalic anhydride (243 mg, 1.0 mmol) in 1,4-dioxane (7 mL). After being refluxed for 4 h under  $\text{N}_2$ , the reaction mixture was allowed to cool to room temperature and concentrated. The residue was purified using flash chromatography (EtOAc/petroleum ether, 4:1 v/v), and **6b** was obtained as a pale yellow solid (130 mg, 45%):  $^1\text{H}$  NMR ( $\text{CDCl}_3$ , 400 MHz)  $\delta$  8.77–8.87 (m, 1H), 8.75–8.76 (m, 1H), 8.71 (d,  $J$  = 8.0 Hz, 1H), 8.42 (t,  $J$  = 8.0 Hz, 1H), 7.98–8.02 (m, 1H), 4.47 (t,  $J$  = 5.4 Hz, 2H), 3.99–4.02 (m, 2H).

**Synthesis of *N*-(2-Hydroxyethyl)-4-amido-1,8-naphthalimide (4).**<sup>21</sup> The preparation process was the same as that used for compound **3** (88%):  $^1\text{H}$  NMR ( $\text{DMSO}-d_6$ , 300 MHz)  $\delta$  8.61 (d,  $J$  = 8.4 Hz, 1H), 8.42 (d,  $J$  = 7.2 Hz, 1H), 8.19 (d,  $J$  = 7.2 Hz, 1H), 7.65 (t,  $J$  = 7.8 Hz, 1H), 7.43 (s, 2H), 6.84 (d,  $J$  = 8.4 Hz, 1H), 4.79 (s, 1H),

4.12 (t,  $J$  = 6.5 Hz, 2H), 3.58 (d,  $J$  = 5.4 Hz, 2H);  $^{13}\text{C}$  NMR ( $\text{DMSO}-d_6$ , 75 MHz)  $\delta$  41.3, 57.9, 107.6, 108.1, 119.3, 121.8, 123.9, 129.2, 129.7, 130.9, 133.9, 152.6, 163.0, 163.9; IR (Nujol)  $\bar{\nu}$  3439 (s), 3352 (s), 3251 (s), 2958 (s), 1632 (m), 1650 (s), 1586 (s), 1380 (s), 774 (s)  $\text{cm}^{-1}$ ; UV/vis (pH 7.0 PBS buffer)  $\lambda_{\text{max}}$  ( $\epsilon$ ) 436 nm ( $11800 \text{ mol}^{-1} \text{ dm}^3 \text{ cm}^{-1}$ ); FTMS (ESI) calcd for  $\text{C}_{14}\text{H}_{13}\text{N}_2\text{O}_3$  [ $\text{M}^+$ ] 257.0921, found 257.0919.

**Synthesis of AcHS-2.** The preparation process was the same as that used for AcHS-1. The reaction mixture was purified by flash column chromatography (EtOAc/petroleum ether, 1:2 v/v) to give AcHS-2 as a pale yellow solid (12 mg, 7.0%):  $^1\text{H}$  NMR ( $\text{CDCl}_3$ , 300 MHz)  $\delta$  = 8.61–8.67 (m, 2H), 8.41 (d,  $J$  = 8.4 Hz, 1H), 8.19 (d,  $J$  = 8.4 Hz, 1H), 7.78 (t,  $J$  = 7.8 Hz, 1H), 7.45–7.50 (m, 3H), 7.07 (d,  $J$  = 8.4 Hz, 2H), 5.27 (s, 2H), 4.56 (t,  $J$  = 6.8 Hz, 2H), 3.84 (t,  $J$  = 6.8 Hz, 2H) ppm;  $^{13}\text{C}$  NMR ( $\text{CDCl}_3$ , 75 MHz)  $\delta$  41.7, 41.4, 67.6, 117.0, 117.6, 119.5, 123.1, 123.2, 126.5, 126.8, 129.2, 130.6, 131.8, 132.1, 133.1, 139.4, 140.9, 153.1, 163.7, 164.3; IR (Nujol)  $\bar{\nu}$  3437 (s), 3290 (s), 3251 (s), 2923 (m), 2115 (s), 1694 (m), 1650 (s), 1538 (s), 1250 (m), 781 (s)  $\text{cm}^{-1}$ ; UV/vis (pH 7.0 PBS buffer)  $\lambda_{\text{max}}$  ( $\epsilon$ ) 373 nm ( $13400 \text{ mol}^{-1} \text{ dm}^3 \text{ cm}^{-1}$ ); TOF-MS ( $\text{ES}^+$ ) calcd for  $\text{C}_{22}\text{H}_{18}\text{N}_5\text{O}_5$  [ $\text{M}^+$ ] 432.1308, found 432.1306.

## ■ ASSOCIATED CONTENT

### ● Supporting Information

Data for detection limits, stability of probes and confocal fluorescence images of cells, and NMR spectra of related compounds. This material is available free of charge via the Internet at <http://pubs.acs.org>.

## ■ AUTHOR INFORMATION

### Corresponding Author

\*E-mail: qhsong@ustc.edu.cn. Fax: (+86) 0551-63601592. Tel: (+86) 0551-63607992.

### Notes

The authors declare no competing financial interest.

## ■ ACKNOWLEDGMENTS

We are grateful for financial support from the National Natural Science Foundation of China (Grant No. 21272224) and the Science Foundation of Anhui Province (128085MB19), facility support from Prof. Jun Wang's laboratory at USTC for cell culture, and Prof. Hongping Zhou of Anhui University for measurements of two-photon excitation spectra of two probes and their sensing products (**3** and **4**).

## ■ REFERENCES

- (1) (a) Li, L.; Rose, P.; Moore, P. K. *Annu. Rev. Pharmacol. Toxicol.* **2011**, *51*, 169–187. (b) Krishnan, N.; Fu, C.; Pappin, D. J.; Tonks, N. K. *Sci. Signal.* **2011**, *4*, ra86.
- (2) (a) Ishigami, M.; Hiraki, K.; Umemura, K. Y.; Ishii, O. K.; Kimura, H. *Antioxid. Redox Signal.* **2009**, *11*, 205–214. (b) Benavides, G. A.; Squadrito, G. L.; Mills, R. W.; Patel, H. D.; Isbell, T. S.; Patel, R. P.; Darley-Usmar, V. M.; Doeller, J. E.; Kraus, D. W. *Proc. Natl. Acad. Sci. U.S.A.* **2007**, *104*, 17977–17982. (c) Singh, S.; Banerjee, R. *Biochim. Biophys. Acta* **2011**, *1814*, 1518–1527.
- (3) Kamoun, P. *Amino Acids*. **2004**, *26*, 243–254.
- (4) Szabó, C. *Nat. Rev. Drug. Discovery* **2007**, *6*, 917–935.
- (5) Kabil, O.; Banerjee, R. *J. Biol. Chem.* **2010**, *285*, 21903–21907.
- (6) (a) Shibuya, N.; Tanaka, M.; Yoshida, M.; Ogasawara, Y.; Togawa, T.; Ishii, K.; Kimura, H. *Antioxid. Redox Signaling* **2009**, *11*, 703–714. (b) Kimura, Y.; Goto, Y.; Kimura, H. *Antioxid. Redox Signaling* **2010**, *12*, 1–13.
- (7) (a) Mari, M.; Morales, A.; Colell, A.; Garcia-Ruiz, C.; Fernandez-Checa, J. C. *Antioxid. Redox Signaling* **2009**, *11*, 2685–2700. (b) Cheng, W. Y.; Tong, H.; Miller, E. W.; Chang, C. J.;

Remington, J.; Zucker, R. M.; Bromberg, P. A.; Samet, J. M.; Hofer, T. P. *Environ. Health Perspect.* **2010**, *118*, 902–908.

(8) (a) Pun, P. B. L.; Lu, J.; Kan, E. M.; Mochhala, S. *Mitochondrion* **2010**, *10*, 83–93. (b) Fu, M.; Zhang, W.; Wu, L.; Yang, G.; Li, H.; Wang, R. *Proc. Natl. Acad. Sci. U.S.A.* **2012**, *109*, 2943–2948.

(9) (a) Zhao, W.; Zhang, J.; Lu, Y.; Wang, R. *EMBO J.* **2001**, *20*, 6008–6016. (b) Wang, R. *FASEB J.* **2002**, *16*, 1792–1798. (c) Kabil, O.; Banerjee, R. *J. Biol. Chem.* **2010**, *285*, 21903–21907. (d) Lavu, M.; Bhushan, S.; Lefer, D. J. *Clin. Sci. (London)* **2011**, *120*, 219–229. (e) Olson, K. R. *Am. J. Physiol.* **2011**, *301*, R297–R312.

(10) For reviews, see: (a) Peng, H.; Chen, W.; Burroughs, S.; Wang, B. *Curr. Org. Chem.* **2013**, *17*, 641–653. (b) Kumar, N.; Bhalla, V.; Kumar, M. *Coord. Chem. Rev.* **2013**, *257*, 2335–2341. (c) Lin, V. S.; Chang, C. J. *Curr. Opin. Chem. Biol.* **2012**, *16*, 595–601. (d) Chan, J. S.; Dodani, C.; Chang, C. J. *Nat. Chem.* **2012**, *4*, 973–984.

(11) (a) Lippert, A. R.; New, E. J.; Chang, C. J. *J. Am. Chem. Soc.* **2011**, *133*, 10078–10080. (b) Peng, H.; Cheng, Y.; Dai, C.; King, A. L.; Predemore, B. L.; Lefer, D. J.; Wang, B. *Angew. Chem., Int. Ed.* **2011**, *50*, 9672–9675. (c) Chen, S.; Chen, Z. J.; Ren, W.; Ai, H.-W. *J. Am. Chem. Soc.* **2012**, *134*, 9589–9592. (d) Yu, F.; Li, P.; Song, P.; Wang, B.; Zhao, J.; Han, K. *Chem. Commun.* **2012**, *48*, 2852–2854. (e) Montoya, L. A.; Pluth, M. D. *Chem. Commun.* **2012**, *48*, 4767–4769. (f) Das, S. K.; Lim, C. S.; Yang, S. Y.; Han, J. H.; Cho, B. R. *Chem. Commun.* **2012**, *48*, 8395–8397. (g) Xuan, W.; Pan, R.; Cao, Y.; Liu, K.; Wang, W. *Chem. Commun.* **2012**, *48*, 10669–10671. (h) Wu, Z.; Li, Z.; Yang, L.; Han, J.; Han, S. *Chem. Commun.* **2012**, *48*, 10120–10122. (i) Wu, M.; Li, K.; Hou, J.; Huang, Z.; Yu, X. *Org. Biomol. Chem.* **2012**, *10*, 8342–8347. (j) Wan, Q.; Song, Y.; Li, Z.; Gao, X.; Ma, H. *Chem. Commun.* **2013**, *49*, 502–504. (k) Sun, W.; Fan, J.; Hu, C.; Zhang, H.; Xiong, X.; Wang, J.; Cui, S.; Sun, S.; Peng, X. *Chem. Commun.* **2013**, *49*, 3890–3892. (l) Bae, S. K.; Heo, C. H.; Choi, D. J.; Sen, D. E.; Joe, H.; Cho, B. R.; Kim, H. M. *J. Am. Chem. Soc.* **2013**, *135*, 9915–9923. (m) Bailey, T. S.; D. Pluth, M. J. *Am. Chem. Soc.* **2013**, *135*, 16697–16704. (n) Zhu, D.; Li, G.; Xue, L.; Jiang, H. *Org. Biomol. Chem.* **2013**, *11*, 4577–4580. (o) Chen, B.; Li, W.; Lv, C.; Zhao, M.; Jin, H.; Jin, H.; Du, J.; Zhang, L.; Tang, X. *Analyst* **2013**, *138*, 946–951. (p) Mao, G.; Wei, T.; Wang, X.; Huan, S.; Lu, D.; Zhang, J.; Zhang, X.; Tan, W.; Shen, G.; Yu, R. *Anal. Chem.* **2013**, *85*, 7875–7881. (q) Li, W.; Sun, W.; Yu, X.; Du, L.; Li, M. *J. Fluoresc.* **2013**, *23*, 181–186. (r) Zhang, H. T.; Wang, P.; Chen, G. C.; Cheung, H.-Y.; Sun, H. Y. *Tetrahedron Lett.* **2013**, *54*, 4826–4829. (s) Zheng, Y.; Zhao, M.; Qiao, Q. L.; Liu, H. Y.; Lang, H. J.; Xu, Z. C. *Dyes Pigments* **2013**, *98*, 367–371. (t) Chen, T.; Zheng, Y.; Xu, Z. C.; Zhao, M.; Xu, Y. G.; Cui, J. N. *Tetrahedron Lett.* **2013**, *54*, 2980–2992. (u) Reja, S. I.; Kumar, N.; Sachdeva, R.; Bhalla, V.; Kumar, M. *RSC Adv.* **2013**, *3*, 17770–17774.

(12) Recent samples: (a) Wang, X.; Sun, J.; Zhang, W.; Ma, X.; Lv, J.; Tang, B. *Chem. Sci.* **2013**, *4*, 2551–2556. (b) Chen, Y.; Zhu, C.; Yang, Z.; Chen, J.; He, Y.; Jiao, Y.; He, W.; Qiu, L.; Cen, J.; Guo, Z. *Angew. Chem., Int. Ed.* **2013**, *52*, 1688–1691. (c) Liu, J.; Sun, Y.; Zhang, J.; Yang, T.; Cao, J.; Zhang, L.; Guo, W. *Chem.—Eur. J.* **2013**, *19*, 4717–4722. (d) Li, X.; Zhang, S.; Cao, J.; Xie, N.; Liu, T.; Yang, B.; He, Q.; Hu, Y. *Chem. Commun.* **2013**, *49*, 8656–8658. (e) Liu, T.; Xu, Z.; Spring, D. R.; Cui, J. *Org. Lett.* **2013**, *15*, 2310–2313. (f) Montoya, L. A.; Pearce, T. F.; Hansen, R. J.; Zakharov, L. N.; Plut, M. D. *J. Org. Chem.* **2013**, *78*, 6050–6064. (g) Chen, X.; Wu, S.; Han, J.; Han, S. *Biol. Med. Chem. Lett.* **2013**, *23*, 5295–5299. (h) Qian, Y.; Yang, B.; Shen, Y.; Du, Q.; Lin, L.; Lin, J.; Zhu, H. *Sens. Actuators B* **2013**, *182*, 498–503. (i) Wang, J. L.; Lin, W. Y.; Li, W. L. *Biomaterials* **2013**, *34*, 7429–7436. (j) Zhang, J. Y.; Sun, Y. Q.; Liu, J.; Shi, Y. W.; Guo, W. *Chem. Commun.* **2013**, *49*, 11305–11307. (k) Liu, T. Y.; Zhang, X. F.; Qiao, Q. L.; Zou, C. Y.; Feng, L.; Cui, J. N.; Xu, Z. C. *Dyes Pigments* **2013**, *99*, 537–542.

(13) Recent samples: (a) Sasakura, K.; Hanaoka, K.; Shibuya, N.; Mikami, Y.; Kimura, Y.; Komatsu, T.; Ueno, T.; Terai, T.; Kimura, H.; Nagano, T. *J. Am. Chem. Soc.* **2011**, *133*, 18003–180035. (b) Qu, X.; Li, C.; Chen, H.; Mack, J.; Guo, Z.; Shen, Z. *Chem. Commun.* **2013**, *49*, 7510–7512.

(14) (a) Wang, B. S.; Li, P.; Yu, F. B.; Song, P.; Sun, X. F.; Yang, S. Q.; Lou, Z. R.; Han, K. L. *Chem. Commun.* **2013**, *49*, 1014–1016. (b) Wang, B. S.; Li, P.; Yu, F. B.; Chen, J. S.; Qu, Z. J.; Han, K. L. *Chem. Commun.* **2013**, *49*, 5790–5792. (c) Lina, V. S.; Lippert, A. R.; Chang, C. J. *PNAS USA* **2013**, *110*, 7131–7135. (d) Wei, L.; Yi, L.; Song, F. B.; Wei, C.; Wang, B. F.; Xi, Z. *Sci. Rep.* **2014**, *4*, 4521. (e) Yuan, L.; Zuo, Q.-P. *Chem.—Asian J.* **2014**, *9*, 1544–1549.

(15) Qian, X.; Xiao, Y.; Xu, Y.; Guo, X.; Qian, J.; Zhu, W. *Chem. Commun.* **2010**, *46*, 6418–6436.

(16) Zhang, J. F.; Lim, C. S.; Bhuniya, S.; Cho, B. R.; Kim, J. S. *Org. Lett.* **2011**, *13*, 1190–1193.

(17) Srikun, D.; Miller, E. W.; Domaille, D. W.; Chang, C. J. *J. Am. Chem. Soc.* **2008**, *130*, 4596–4597.

(18) Robinson, A.-M.; Evers, E. L.; Griffin, R. J.; Irwin, W. J. *J. Pharm. Pharmacol.* **1988**, *40*, 61P.

(19) (a) Cava, M. P.; Merkel, K. E.; Schlessinger, R. H. *Tetrahedron* **1965**, *21*, 3059–3064. (b) Dong, M.; Wang, Y. W.; Peng, Y. *Org. Lett.* **2010**, *12*, 5310–5313.

(20) Wu, J.; Huang, R.; Wang, C. C.; Liu, W. T.; Wang, J. Q.; Weng, X. C.; Tian, T.; Zhou, X. *Org. Biomol. Chem.* **2013**, *11*, 580–585.

(21) Zhang, J. F.; Kim, S.; Han, J. H.; Lee, S.-J.; Pradhan, T.; Cao, Q. Y.; Lee, S. J.; Kang, C.; Kim, J. S. *Org. Lett.* **2011**, *13*, 5294–5297 and references therein.

(22) Perrin, D. D. *Ionization Constants of Inorganic Acids and Bases in Aqueous Solution*, 2nd ed.; Pergamon: Oxford, 1982.

(23) (a) Dombkowski, R. A.; Russell, M. J.; Olson, K. R. *Am. J. Physiol.* **2004**, *286*, R678–R685. (b) Hughes, M. N.; Centelles, M. N.; Moore, K. P. *Free Radical Biol. Med.* **2009**, *47*, 1346–1353.

(24) *A Guide to Fluorescent Probes and Labeling Technologies*, 11th ed.; Johnson, I., Spence, M. T. Z., Eds.; The Molecular Probes: Eugene, OR, 2010.

(25) Demas, J. N.; Crosby, J. A. *J. Phys. Chem.* **1971**, *73*, 991–1024.

(26) Dawson, W. R.; Windsor, M. W. *J. Phys. Chem.* **1968**, *72*, 3251–3260.

(27) Ji, Z.; Li, Y.; Pritchett, T. M.; Makarov, N. S.; Haley, J. E.; Li, Z.; Drobizhev, M.; Rebane, A.; Sun, W. *Chem.—Eur. J.* **2011**, *17*, 2479–2491.

(28) Zheng, Q.; He, G. S.; Prasad, P. N. *J. Mater. Chem.* **2005**, *15*, 579–587.

(29) Li, D. M.; Zhang, Q.; Wang, P.; Wu, J. Y.; Kan, Y. H.; Tian, Y. P.; Zhou, H. P.; Yang, J. X.; Tao, X. T.; Jiang, M. H. *Dalton Trans.* **2011**, *40*, 8170–8178.

(30) Fan, J.; Sun, W.; Hu, M.; Cao, J.; Cheng, G.; Dong, H.; Song, K.; Liu, Y.; Sun, S.; Peng, X. *Chem. Commun.* **2012**, *48*, 8117–8119.